arXiv:1304.0262v2 [cond-mat.stat-mech] 12 Dec 2013

Carnot cycle at finite power: Attainability of maximal efficiency

Armen E. Allahverdyan,[1] Karen V. Hovhannisyan,[2,1] Alexey V. Melkikh,[3] and Sasun G. Gevorkian[4]
[1] *Yerevan Physics Institute, Alikhanian Brothers Street 2, Yerevan 375036, Armenia*
[2] *ICFO-Institut de Ciències Fotòniques, Mediterranean Technology Park, 08860 Castelldefels (Barcelona), Spain*
[3] *Ural Federal University, Mira Street 19, Yekaterinburg 620002, Russia and*
[4] *Institute of Physics, Academia Sinica, Nankang, Taipei 11529, Taiwan*

We want to understand whether and to which extent the maximal (Carnot) efficiency for heat engines can be reached at a finite power. To this end we generalize the Carnot cycle so that it is not restricted to slow processes. We show that for realistic (i.e. not purposefully-designed) engine-bath interactions, the work-optimal engine performing the generalized cycle close to the maximal efficiency has a long cycle time and hence vanishing power. This aspect is shown to relate to the theory of computational complexity. A physical manifestation of the same effect is the Levinthal's paradox in the protein folding problem. The resolution of this paradox for realistic proteins allows to construct engines that can extract at a finite power 40 % of the maximally possible work reaching 90 % of the maximal efficiency. For purposefully designed engine-bath interactions, the Carnot efficiency is achievable at a large power.

PACS numbers: 05.20.-y, 05.10.Gg, 05.70.Ln

Reciprocating heat engines extract work operating cyclically between two thermal baths at temperatures T_1 and T_2 ($T_1 > T_2$) [1]. They have two basic characteristics: *(i)* efficiency, $\eta = W/Q_1$, is the work W extracted per cycle divided by the heat input Q_1 from the high-temperature bath. *(ii)* Power W/τ, where τ is the cycle duration. Both these quantities have to be large for a good engine: if η is small, lot of energy is wasted; if the power is small, no sizable work is delivered over a reasonable time [1].

The second law establishes the Carnot efficiency $\eta_{\rm C} = 1 - \frac{T_2}{T_1}$ as an upper bound for η [1]. The Carnot cycle reaches the bounding value $\eta_{\rm C}$ in the (useless) limit, where the power goes to zero [1]. Conversely, realistic engines are not efficient, since they have to be powerful, e.g. the efficiency of Diesel engines amounts to 35–40 % of the maximal value. This *power-efficiency dilemma* motivated a search for the efficiency that would generally characterize the maximal power regime. One candidate for this is the Curzon-Ahlborn efficiency $\eta_{\rm CA} = 1 - \sqrt{T_2/T_1}$ [2], which is however crucially tied to the linear regime $T_1 \approx T_2$ [3, 4]. Beyond this regime $\eta_{\rm CA}$ is a lower bound of η for a class of model engines [5]. Several recent models for the efficiency at the maximal power overcome $\eta_{\rm CA}$ with $\eta^* = \frac{\eta_{\rm C}}{2-\eta_{\rm C}}$ [6].

As argued in [5, 7, 8], the maximal power regime allows for the Carnot efficiency, at least for certain models. But it is currently an open question whether the maximal efficiency is attained under realistic conditions (see e.g. [9] versus [7]), and how to characterize the very *realism* of those conditions. Even more generally: what is the origin of the power-efficiency dilemma? We answer these questions by analyzing a generalized Carnot cycle, which in contrast to the original Carnot cycle is not restricted to slow processes. We now summarize our answers.

(1) When the N-particle engine operates at the maximal work extracted per cycle, its efficiency reaches the Carnot bound $\eta_{\rm C}$ for $N \gg 1$, while the cycle time is given by the relaxation time of the engine. The maximal work and the Carnot efficiency are achieved due to the flat energy landscape of the engine. For realistic engine-bath interactions this energy landscape leads to a very long [$\mathcal{O}(e^N)$] relaxation time nullifying the power. By realistic we mean interactions that are independent from the engine Hamiltonian. If we assume a proper tuning between engine-bath interaction and the engine Hamiltonian, the relaxation time scales as $\mathcal{O}(\sqrt{N})$, and the maximal efficiency is achievable in the limit $N \gg 1$ at a large power $\mathcal{O}(\sqrt{N})$.

(2) The relaxation of the optimal engine under realistic interactions relates to an important problem of searching an unstructured database for a marked item, where each energy level refers to a database item. This task is computationally complex, i.e. even the most powerful quantum algorithms resolve it in $\mathcal{O}(e^{N/2})$ time-steps [11]. Hence the power-efficiency dilemma relates to computational complexity. The same effect can be reformulated as the Levinthal's paradox of the protein folding problem: if the majority of unfolded states of a protein are assumed to have the same (free) energy, the folding time is very long [14].

(3) A scenario of resolving the Levinthal's paradox proposed in protein science shows the way of constructing sub-optimal engines that operate at a reasonably large values of work, power and efficiency. These sub-optimal engines function as model proteins, but they are restricted to mesoscopic scales $N \sim 100$; otherwise the relaxation time is again large. Sacrificing some 50–60% of the maximal possible work leads to a reasonable cycle times with the efficiency that achieves some 90 % of the maximal (Carnot) efficiency.

Carnot cycle and its generalization. Recall that the Carnot cycle consists of four slow, consecutive pieces [1]: thermally-isolated – isothermal – thermally-isolated – isothermal. Four times slow brings in the vanishing power stressed above; see additionally section I of the

Supplementary Material. Since the overall process is a quasi-equilibrium one, the external fields that extract work from the engine act on it during all the four pieces. One deduces for the isothermal parts: $Q_1 = T_1\Delta S$ and $Q_2 = T_2\Delta S$, where Q_1 (Q_2) is the heat taken from (put into) the T_1-bath (T_2-bath), and $\Delta S > 0$ is the entropy change. Since the work extracted is $W = Q_1 - Q_2$, η equals to its maximal value $\eta_{\rm C} = 1 - \frac{T_2}{T_1}$ [1].

We keep the two isothermal and two thermally isolated pieces of the original Carnot cycle, but do not force them to be slow. In addition, the external fields will act only during the thermally isolated stages. Isothermal pieces amount to free relaxation. Due to these points, we can analyze the engine functioning from the energy conservation. We study the engine via quantum mechanics on a finite Hilbert space, because this reduces the problem to a combinatorial optimization. The final results are interpreted classically and can be also obtained by discretizing the Hamiltonian classical dynamics over phase-space cells.

0. The engine E with the Hamiltonian H_1 starts in an equilibrium state at temperature T_1 described by the density matrix

$$\rho(0) = \rho_1 = e^{-\beta_1 H_1}/({\rm tr}\, e^{-\beta_1 H_1}), \quad \beta_1 = 1/T_1. \qquad (1)$$

1. Between times 0 and τ, E undergoes a thermally isolated process with a time-dependent Hamiltonian $H_{12}(t)$ and the unitary evolution $\rho(\tau) = U_{12}\rho(0)U_{12}^\dagger$:

$$H_{12}(0) = H_1, \quad H_{12}(\tau) = H_2, \quad U_{12} = \mathcal{T} e^{-i\int_0^\tau {\rm d}s H_{12}(s)}, \qquad (2)$$

where $\mathcal{T}$ means chronological ordering. The work taken out of E is determined by energy conservation (see [1] and section II of the Supplementary Material)

$$W_1 = {\rm tr}[H_1\rho_1 - H_2 U_{12}\rho_1 U_{12}^\dagger]. \qquad (3)$$

2. Then E is attached to the T_2-bath and after relaxation time $\tau_{\rm r}$ its density matrix becomes

$$\rho(\tau + \tau_{\rm r}) = \rho_2 = e^{-\beta_2 H_2}/({\rm tr}\, e^{-\beta_2 H_2}). \qquad (4)$$

The heat that came to E from the T_2-bath is

$$Q_2 = {\rm tr}[H_2\rho_2 - H_2 U_{12}\rho_1 U_{12}^\dagger]. \qquad (5)$$

3. E undergoes another thermally isolated process

$$H_{21}(0) = H_2, \quad H_{21}(\tau) = H_1, \quad U_{21} = \mathcal{T} e^{-i\int_0^\tau {\rm d}s H_{21}(s)}, \qquad (6)$$

completing the cycle with respect to the Hamiltonian. The work taken out of E reads

$$W_2 = {\rm tr}[H_2\rho_2 - H_1 U_{21}\rho_2 U_{21}^\dagger]. \qquad (7)$$

4. Finally, E is attached to the T_1-bath ($T_1 > T_2$) and relaxes to ρ_1 thereby completing the cycle; see (1). The heat that came to E from the T_1-bath is

$$Q_1 = {\rm tr}[H_1\rho_1 - H_1 U_{21}\rho_2 U_{21}^\dagger]. \qquad (8)$$

To stress the differences with the original Carnot cycle: *(i)* the cycle time $2(\tau + \tau_{\rm r})$ need not be much larger than the relaxation time $\tau_{\rm r}$. *(ii)* The cycle is out of equilibrium. *(iii)* The work source and the bath never act simultaneously; either one acts or another. Hence heat and work are deduced from the energy conservation.

We did not count the work necessary for switching the system-bath interaction on and o ff, because we assume that it does not contribute to the total work budget (e.g. since it is weak).

Maximization of work. We maximize the full extracted work $W = W_1 + W_2$ over H_1, H_2, U_{12}, U_{21} for fixed $T_1 > T_2$ and a fixed number $n+1$ of energy levels of E. The lowest energies of H_1 and H_2 can be set to zero. Introduce the eigen-resolution of H_α

$$H_\alpha = \sum\nolimits_{k=2}^{n+1} \epsilon_k^{[\alpha]} |k^{[\alpha]}\rangle\langle k^{[\alpha]}|, \quad \alpha = 1, 2. \qquad (9)$$

The full work $W = W_1 + W_2$ reads from (3, 7)

$$W = \sum\nolimits_{\alpha=1}^{2} \sum\nolimits_{k=2}^{n+1} p_k^{[\alpha]} \epsilon_k^{[\alpha]} \qquad (10)$$

$$- \sum\nolimits_{k,l=2}^{n+1} \left[p_k^{[2]} \epsilon_l^{[1]} C_{kl}^{[21]} + p_k^{[1]} \epsilon_l^{[2]} C_{kl}^{[12]} \right], \qquad (11)$$

where $\{p_k^{[\alpha]}\}_{k=1}^{n+1}$ are eigenvalues of ρ_α given by (1, 4, 9), and where

$$C_{kl}^{[\alpha\gamma]} \equiv |\langle k^{[\alpha]} | U_{\alpha\gamma} | l^{[\gamma]}\rangle|^2, \quad (\alpha, \gamma) = (1, 2), (2, 1). \qquad (12)$$

$C_{kl}^{[\alpha\gamma]}$ are doubly stochastic matrices: $\sum_{k=1}^{n+1} C_{kl}^{[\alpha\gamma]} = \sum_{l=1}^{n+1} C_{kl}^{[\alpha\gamma]} = 1$. Such a matrix C_{kl} can be represented as a convex sum of permutation matrices (Birkhoff's theorem) [12]: $C_{kl} = \sum_\delta \lambda_\delta \Pi_{kl}^{[\delta]}$, where $\lambda_\delta \geq 0$, $\sum_\delta \lambda_\delta = 1$, and where $\Pi^{[\delta]}$ permutes the components of any vector on which it acts. Hence we can maximize W in (10, 11) over $\{\lambda_\delta\}$. The optimal $C_{kl}^{[12]}$ and $C_{kl}^{[21]}$ amount to permutation matrices, since $\{\lambda_\delta\}$ enter linearly into W. Without loss of generality we can assume $\epsilon_1^{[\alpha]} \leq ... \leq \epsilon_{n+1}^{[\alpha]}$ and hence $p_1^{[\alpha]} \geq ... \geq p_{n+1}^{[\alpha]}$. Then the optimal permutations $C_{kl}^{[12]}$ and $C_{kl}^{[21]}$ are unit matrices; see (11). In contrast to the original Carnot cycle, the optimal thermally isolated processes can be realized as sudden (quick) changes of the Hamiltonian eigenvalues without changing the eigenvectors. A prominent example of such a process is the Mössbauer effect [17]. It is an advantage that thermally isolated processes can be fast; otherwise it is difficult to maintain thermal isolation, which is a known problem of the original Carnot cycle [1].

The work

$$W = W_1 + W_2 = \sum\nolimits_{k=2}^{n+1} (p_k^{[1]} - p_k^{[2]})(\epsilon_k^{[1]} - \epsilon_k^{[2]}), \qquad (13)$$

is to be still maximized over $\{\epsilon_k^{[1]}\}_{k=2}^{n+1}$ and $\{\epsilon_k^{[2]}\}_{k=2}^{n+1}$; see (12). W is symmetric with respect to permutations within $\{\epsilon_k^{[1]}\}_{k=2}^{n+1}$ and within $\{\epsilon_k^{[2]}\}_{k=2}^{n+1}$. We checked numerically that this symmetry is not broken and hence

the maximum of W is reached for

$$\epsilon^{[\alpha]} \equiv \epsilon_2^{[\alpha]} = ... = \epsilon_{n+1}^{[\alpha]}, \quad \alpha = 1, 2, \tag{14}$$

i.e. all excited levels have the same energy. Thus the thermally isolated pieces of the cycle consist, respectively, of sudden changes $\epsilon^{[1]} \to \epsilon^{[2]}$ and $\epsilon^{[2]} \to \epsilon^{[1]}$.

With new variables $e^{-\beta_\alpha \epsilon^{[\alpha]}} \equiv u_\alpha$ we write the maximal work as

$$W_{\max}[u_1, u_2] = \frac{(T_1 \ln \frac{1}{u_1} - T_2 \ln \frac{1}{u_2})(u_1 - u_2)n}{[1 + nu_1][1 + nu_2]}, \tag{15}$$

where u_1 and u_2 are found from

$$\partial_{u_1} W_{\max}[u_1, u_2] = \partial_{u_2} W_{\max}[u_1, u_2] = 0. \tag{16}$$

u_1 and u_2 depend on T_2/T_1 and on n. Noting (8) and the result before (13) we obtain $Q_1 = \mathrm{tr}(H_1(\rho_1 - \rho_2))$ for the heat obtained from the high-temperature bath. Using (14) we get from $\eta = W/Q_1$ and from (15):

$$\eta = 1 - [T_2 \ln u_2] / [T_1 \ln u_1] \, . \tag{17}$$

Note from (15) that $W_{\max}[u_1, u_2] > 0$ and $T_2 < T_1$ imply $1 > \epsilon^{[2]}/\epsilon^{[1]} > T_2/T_1$. Hence (17) implies $\eta \leq \eta_{\mathrm{C}} = 1 - T_2/T_1$, as expected.

Both $W_{\max}[u_1, u_2]$ and η increase with n. For $\ln[n] \gg 1$ we get asymptotically from (16):

$$u_1 = \frac{(1-\theta)\ln[n]}{n}, \qquad u_2 = \frac{\theta}{n \ln[n](1-\theta)}, \tag{18}$$

where $\theta \equiv T_2/T_1$. This produces

$$W_{\max}[u_1, u_2] = (T_2 - T_1)\ln[n] - \mathcal{O}(1/\ln[n]), \tag{19}$$

$$\eta = \eta_{\mathrm{C}} - \mathcal{O}(1/\ln[n]), \quad \eta_{\mathrm{C}} \equiv 1 - T_2/T_1. \tag{20}$$

The maximal work $W_{\max}[u_1, u_2]$ scales as $\ln[n]$, since this is the "effective number of particles" for the engine. In the macroscopic limit $\ln[n] \gg 1$, the efficiency converges to its maximal value $\eta_{\mathrm{C}} = 1 - T_2/T_1$; see (20).

The cycle time amounts to two times the relaxation time τ_{r} of the system with spectrum (14) and energy gap $\epsilon \sim \ln[n]$; see (14, 18). (Recall that the thermally isolated stages of the cycle are very quick.) The magnitude of τ_{r} essentially depends on the scenario of relaxation.

First (specific) scenario. We can assume that the Hamiltonian (9, 14) of the heat engine is known. Then there exist system-bath interaction scenarios that generally produce a non-Markovian dynamics of the system and lead to $\tau_{\mathrm{r}} = \mathcal{O}(\sqrt{\ln[n]})$; see sections VI and VII of the Supplementary Material. Hence for this type of relaxation the Carnot efficiency is achievable at a large power $\mathcal{O}(\sqrt{\ln[n]}) \gg 1$; see (19). However, in these scenarios the system-bath interaction Hamiltonian (that governs the relaxation) is special: it depends on the engine Hamiltonian (9, 14).

Second (realistic) scenario. Assuming that the system-bath interaction does not depend on the Hamiltonian (9, 14), we can estimate τ_{r} within the weak-coupling, Markov master equation approach that leads to $\tau_{\mathrm{r}} = \mathcal{O}(n)$; see section III of the Supplementary Material. For a qualitative understanding of this situation, consider the relaxation as a random walk in the energy space, e.g. in the second step of the cycle, where the engine starts with almost unpopulated ground state, and it has to achieve ground state probability ≈ 1 after relaxation; see (18). So, if every transition from one excited energy level to another takes a finite time, one will need to perform in average $n/2$ transitions before jumping to the ground state. Now note from (20) that the convergence of η to η_{C} is controlled by $\mathcal{O}(1/\ln[n])$: a small step towards η_{C} will lead to a large increase in τ_{r} nullifying the power $\mathcal{O}(\ln[n]/n)$ for $n \gg 1$; see (19). Hence for this type of relaxation the Carnot efficiency is not achievable at a finite power.

The second relaxation scenario of the system with Hamiltonian (9, 14) is similar to the known combinatorial optimization problem: finding a marked item in an unstructured database [11] of $n + 1$ items. This problem is mapped to physics by associating each item to an eigenvector of a Hamiltonian [11]. The marked item relates to the lowest energy level 0, while all other (excited) eigenvalues of the Hamiltonian ϵ are equal. The resulting system has unknown eigenvectors of the Hamiltonian, but known eigenenergies. Now the searching process can be organized as a relaxation of the system from an excited state to a low-temperature equilibrium state. This state is dominated by the ground level due to a large ϵ. Once the relaxation is over, the unknown item (eigenvector) can be revealed by measuring the energy [15].

For classical algorithms the search time of this problem scales as $\mathcal{O}(n)$ for $n \gg 1$ [11]. It is thus not much better than going over all possible candidates for the solution, a typical situation of a computationally complex problem. For quantum algorithms (Grover's search) the search time scales as $\mathcal{O}(\sqrt{n})$ [11]. This is still not suitable for our purposes, since it nullifies the power for $\ln[n] \gg 1$.

Sub-optimal engine. Within the second (realistic) relaxation scenario, we shall modify the optimal engine so that the power is finite, but both the work and efficiency are still large. We are guided by the analogy between the relaxation of the Hamiltonian (9, 14) under the second scenario and the Levinthal's paradox from protein physics [14]. In fact, (9, 14) is the simplest model employed for illustrating the paradox; see [13, 14] and section V of the Supplementary Material. Here the ground state refers to the unique folded (native) state. To ensure its stability, it is separated by a large gap from excited (free) energy levels. The essence of the paradox is that assuming many *equivalent* unfolded (excited) states, the relaxation time to the native state is unrealistically long. Recall that the states ρ_1 and ρ_2 of the optimal engine refer respectively to unfolded and folded states of the protein model. Indeed $nu_\alpha/(1 + nu_\alpha)$ $(\alpha = 1, 2)$ is the overall probability of the excited levels; see (14). Hence for $\ln[n] \gg 1$ the ground state (excited levels) dominates in ρ_2 (ρ_1); see (18).

The resolution of the paradox is to be sought via resolving the degeneracy of excited levels: if there are energy differences, some (unfavorable) transitions will not be made shortening the relaxation time [13, 14]. In resolving the energy degeneracy we follow the simplest model proposed in [14].

The model has $N \gg 1$ degrees of freedom $\{\sigma_i\}_{i=1}^n$; each one can be in $\zeta+1$ states: $\sigma_i = 0, ..., \zeta$. Whenever $\sigma_i = 0$ for all i's, the model protein is in the folded (ground) state with energy zero [13, 14]. The ground state has zero energy. Excited states with $s \geq 1$ have energy $\epsilon + \delta s$, where $\epsilon > 0$ and s is the number of (misfolded) degrees of freedom with $\sigma_i \neq 0$. $\delta > 0$ is the parameter that (partially) resolves the degeneracy of excited states; we revert to the previous, work-optimal, model for $\delta \to 0$. For *different* eigenvalues of the Hamiltonian H_α we have

$$\left\{ \left(1 - \delta_{\rm Kr}[s,0]\right) \left(\epsilon^{[\alpha]} + s\delta^{[\alpha]}\right) \right\}_{s=0}^{N}, \quad \alpha = 1, 2, \qquad (21)$$

where $\delta_{\rm Kr}[s,0]$ is the Kronecker delta, and where each energy $\epsilon^{[\alpha]} + s\delta^{[\alpha]}$ is degenerate $\frac{\zeta^s N!}{s!(N-s)!}$ times; thus the total number of energy levels is $(1+\zeta)^N$.

Given (21), the cycle consists of two isothermal and two thermally isolated pieces with sudden changes $(\delta^{[1]}, \epsilon^{[1]}) \to (\delta^{[2]}, \epsilon^{[2]}) \to (\delta^{[1]}, \epsilon^{[1]})$; see (1–13). Below we shall also assume

$$\beta_1 \delta^{[1]} = \beta_2 \delta^{[2]}, \qquad (22)$$

because this makes the sub-optimal engine structurally very similar to the optimal one. Now the work $W = W_1 + W_2$ is calculated from (3, 7, 8, 21, 22):

$$W[v_1, v_2; K] = \frac{m(\Delta\epsilon + \frac{KN\Delta\delta}{1+K})(v_1 - v_2)}{(1+mv_1)(1+mv_2)}, \qquad (23)$$

$$\Delta\epsilon = \epsilon^{[1]} - \epsilon^{[2]} = T_1 \ln[1/v_1] - T_2 \ln[1/v_2], \qquad (24)$$

$$\Delta\delta = \delta^{[1]} - \delta^{[2]} = (T_1 - T_2) \ln[\zeta/K]. \qquad (25)$$

where $K = \zeta e^{-\beta_1 \delta^{[1]}}$, $m = (1+K)^N$, and where $v_\alpha \equiv e^{-\beta_\alpha \epsilon^{[\alpha]}}$ $(\alpha = 1, 2)$ are determined from maximizing (23). Note the analogy between (15) and (23), with m being an analogue of n; they get equal for $\delta \to 0$. Note that in (23) we neglected factor $\mathcal{O}(\frac{1}{m})$ assuming that $m \gg 1$.

Likewise, we get for the efficiency [cf. (17)]:

$$\eta = 1 - \frac{T_2}{T_1} \times \frac{\ln \frac{1}{v_2} + \frac{NK \ln(\zeta/K)}{1+K}}{\ln \frac{1}{v_1} + \frac{NK \ln(\zeta/K)}{1+K}}. \qquad (26)$$

For this model [14] assumes a local Markov relaxation dynamics, where each degree of freedom makes a transition $\sigma_i \to \sigma_i \pm 1$ in 10^{-9} seconds; this value is chosen conventionally to fit experimental magnitudes for the elementary dynamic step [14]. The model has a single relaxation time [14] that is easily reproduced in the general master-equation framework (see section IV of the Supplementary Material):

$$\tau_{\rm r} = 10^{-9}(1+K)^N/(NK) \text{ seconds}, \qquad (27)$$

TABLE I: Parameters of the sub-optimal engine: work W, efficiency η and the cycle time $2\tau_{\rm r}$; see (23–C). $W_{\max}$ is the maximal work extracted for the optimal engine at a vanishing power; see (15, 16). For the sub-optimal engine: $K = \zeta e^{-\beta_1 \delta^{[1]}}$, $N = 140$, $\zeta = 4$, $T_1 = 1$, $T_2 = 1/2$. Carnot and Curzon-Ahlborn efficiencies are, respectively, $\eta_{\rm C} = 1/2$ and $0.5858\,\eta_{\rm C}$. Also, $p_1^{[\alpha]} = [1+(1+K)^N e^{-\beta_\alpha \epsilon^{[\alpha]}}]^{-1}$ $(\alpha = 1, 2)$ are the ground-state probabilities of $\rho_\alpha \propto e^{-\beta_\alpha H_\alpha}$; see (21).

K	$\tau_{\rm r}$	$W/W_{\max}$	W	$\eta/\eta_{\rm C}$	$p_1^{[1]}$	$p_1^{[2]}$
0.1	4.45×10^{-5} s	0.2267	23.52	0.8751	0.0392	0.9808
0.2	4.35 s	0.3884	40.3	0.9110	0.0237	0.9883
0.24	357 s	0.4393	45.58	0.9181	0.0210	0.9896

where the factor N is due to the N-times degenerate first excited level.

For $\delta^{[\alpha]} \to 0$ $(\alpha = 1, 2)$, where the excited energy levels become degenerate, $\tau_{\rm r} \propto (1+\zeta)^N$ scales linearly over the number of energy levels, as expected. When $\delta^{[\alpha]}$ are not zero, $\tau_{\rm r}$ can be of order of 1 second for $N \sim 100$, because $1+K$ is close to 1. However, for the macroscopic situation ($N \sim 10^{23}$) $\tau_{\rm r}$ is still huge. In this sense, the model is incomplete, but still useful for analyzing the mesoscopic situation $N \sim 100$ that is relevant for the protein folding problem [13].

Table I illustrates the characteristics of the sub-optimal engine and compares them with those of the optimal one. Reasonable cycle times can coexist with a finite fraction ($\sim 40\%$) of the maximal work and with sizable efficiencies ($\sim 90\%$ of the maximal value) that are larger than the Curzon-Ahlborn value. Hence, albeit within the second (realistic) scenario it is impossible to approach the maximal efficiency as close as desired, reasonably large efficiencies at a finite (or even large) power are possible. These results resemble the power-efficiency trade-off (see [10]), but they are more complicated, since they involve work, efficiency and power.

K.V.H. is supported by the Spanish project FIS2010-14830. S.G.G. is supported by Grant NSC 101-2811-M-001-156.

[1] H.B. Callen, *Thermodynamics* (John Wiley, NY, 1985).

[2] J. Yvon, *The Saclay reactor*, Proceedings of the Interna-

tional Conference on Peaceful uses of Atomic Energy. p. 387, Geneva (1955).
P. Chambadal, *Les Centrales Nucléaires* (Armand Colin, Paris, France, 1957).
I. I. Novikov, J. Nuclear Energy II **7**, 125 (1958).
F. Curzon and B. Ahlborn, Am. J. Phys. **43**, 22 (1975).
[3] C. Van den Broeck, Phys. Rev. Lett. **95**, 190602 (2005).
[4] M. Esposito, K. Lindenberg and C. Van den Broeck, Phys. Rev. Lett. **102**, 130602 (2009).
[5] A.E. Allahverdyan, R.S. Johal, and G. Mahler, Phys. Rev. E **77**, 041118 (2008)
[6] See, e.g., M. Esposito, R. Kawai, K. Lindenberg, and C. Van den Broeck, Phys. Rev. Lett. **105**, 150603 (2010).
[7] G. Benenti, K. Saito, and G. Casati, Phys. Rev. Lett. **106**, 230602 (2011).
[8] U. Seifert, Phys. Rev. Lett. **106**, 020601 (2011).
[9] K. Brandner, K. Saito, and U. Seifert, Phys. Rev. Lett. **110**, 070603 (2013).
[10] B. Jiménez de Cisneros and A.C. Hernández, Phys. Rev. Lett. **98**, 130602 (2007).
[11] E. Farhi and S. Gutmann, Phys. Rev. A **57**, 2403 (1998).
[12] A.W. Marshall and I. Olkin, *Inequalities: Theory of Majorization and its Applications* (Academic Press, NY, 1979).
[13] K. Sneppen and G. Zocchi, *Physics in Molecular Biology* (Cambridge University Press, Cambridge, 2005).
[14] R. Zwanzig, PNAS, **92**, 9804 (1995).
[15] Since the full Hamiltonian is not uknown this measurement will at least take $\hbar/(\delta\epsilon)$ seconds due to the energy-time uncertainty principle, where $\delta\epsilon$ is the precision by which the ground-state energy is measured; see [16]. This time is however a small overhead to the search time.
[16] Y. Aharonov, S. Massar and S. Popescu, Phys. Rev. A **66**, 052107 (2002).
[17] A. B. Migdal, *Qualitative methods in quantum theory* (Westview Press, 2000).

Supplementary Material

This material consists of seven sections. Almost all of them can be read independently.

Section A clarifies the finite power condition for the generalized Carnot cycle and it compares it with the usual Carnot cycle.

Section B relates together two definitions of (thermodynamical) work.

Section C estimates the relaxation time of the optimal engine within the master-equation framework. Since this is one of the main points of the present work, we dwell on it in detail and spell out all (hidden) assumptions necessary for its derivation. Section D presents a similar estimation for the sub-optimal engine.

In section E we discuss the current status of the Levinthal's paradox within the protein folding theory.

Section F discusses an example of the quantum relaxation scenario, where the system-bath interaction is engineered, i.e., it correlates with the system Hamiltonian. We show that the relaxation time of the optimal engine within this scenario is short. Due to this fact, the Carnot efficiency can be reached at a large power. Finally, in section G we show that this shortening of the relaxation time is not related to the extensive usage of resources such as quantum entanglement.

Appendix A: Power for the (generalized) Carnot cycle

Here we discuss in some details the power of the generalized Carnot cycle and compare this situation with the usual Carnot cycle.

Recall from the main text that the generalized Carnot cycle consists of four pieces: two of them are thermally isolated that can proceed very fast. The rate-limiting steps are the two pieces with free relaxation, since their duration is bound by the relaxation time.

To achieve a cyclic process within the exponential relaxation with the relaxation time $\tau_{\rm r}$, the cycle time τ should be larger than $\tau_{\rm r}$. For each cycle the deviation of the post-relaxation state from the exact equilibrium (Gibbsian) state will be of order $e^{-\tau/\tau_{\rm r}}$. Thus if the ratio $\tau/\tau_{\rm r}$ is simply large, but finite, one can perform roughly $\sim e^{\tau/\tau_{\rm r}} \gg 1$ number of cycles at a finite power, before deviations from cyclicity would accumulate and the machine will need resetting.

The above situation does differ from the power consideration of usual (reversible) thermodynamic cycles, e.g., the Carnot cycle [6–8]. There the external fields driving the machine through various stages have to be much slower than the relaxation to the momentary equilibrium. The latter means that the machine is described by its equilibrium Gibbs distribution with time-dependent parameters. In particular, the condition of momentary equilibrium for the working medium is necessary for the Carnot cycle to reach the Carnot efficiency [6].

The precise meaning of the external fields being slow is important here. If $\tau_{\rm F}$ is the characteristic time of the fields, then the deviations from the momentary equilibrium are of order $\mathcal{O}[\frac{\tau_{\rm r}}{\tau_{\rm F}}]$ [6–8]. This fact is rather general and does not depend on details of the system and of the studied process, e.g., it does not depend whether the process is thermally isolated or adiabatic. In particular, it is this deviation of the state from the momentary equilibrium that brings in the entropy production (or work dissipation) of order of $\mathcal{O}[\left(\frac{\tau_{\rm r}}{\tau_{\rm F}}\right)^2]$ [6–8].

Thus performing the reversible Carnot cycle with (approximately) the Carnot efficiency means keeping the ratio $\frac{\tau_{\rm r}}{\tau_{\rm F}}$ very small.

Here are the differences between the Carnot cycle and our situation:

- In our case we do not require the machine to be close to its momentary equilibrium state during the whole process. It suffices that the machine gets enough time to relax to its final equilibrium.

- A small, but finite $\frac{\tau_{\rm r}}{\tau_{\rm F}}$ for the Carnot cycle situation means that deviations from the momentary

equilibrium are visible already within one cycle. In contrast, a small, but finite $\frac{\tau_r}{\tau}$ for our situation means that we can perform an exponentially large number of cycles before deviations from the cyclicity will be sizable. Here is a numerical example. Assume that $\frac{\tau_r}{\tau} = \frac{\tau_r}{\tau_F} = 1/20$. For the standard Carnot cycle already within one cycle the deviation from the momentary equilibrium will amount to 0.05. In our situation the same amount $e^{-3} = 0.0498$ of deviation from the cyclicity will come after $e^{17} = 2.4 \times 10^7$ cycles. This is a large number, especially taking into account that no realistic machine is supposed to work indefinitely long. Such machines do need resetting or repairing. The point is that our machine can perform *many* cycles at a finite power before any resetting is necessary.

Appendix B: Clarification of the concept of work as used in our situation.

Let a system interact with a source of work only (thermally isolated process). This means that the system Hamiltonian $H[\alpha(t)]$ is a function of a (classical) parameter $\alpha(t)$. The work done on the system per unit of time equals to "force" times "displacement" and averaged over state of the system, as represented by a time-dependent density matrix $\rho(t)$:

$$\frac{\mathrm{d}W}{\mathrm{d}t} = \frac{\mathrm{d}\alpha(t)}{\mathrm{d}t}\mathrm{tr}\left(\frac{\partial H}{\partial \alpha}\rho(t)\right). \tag{B1}$$

The same formula applies in the classical situation, where tr means integration over the phase-space (the space of coordinates and momenta), while ρ becomes the phase-space probability density. Now one can use the equations of motion for the density matrix, $i\hbar\frac{\mathrm{d}\rho}{\mathrm{d}t} = H[\alpha(t)]\rho(t) - \rho(t)H[\alpha(t)]$ (in the classical situation this becomes the Liouville equation), to show from (B1) that the total work equals to the change of average energy

$$W(\tau) = \int_0^\tau \mathrm{d}t\,\frac{\mathrm{d}W}{\mathrm{d}t} = \mathrm{tr}\left(H[\alpha(\tau)]\rho(\tau) - H[\alpha(0)]\rho(0)\right). \tag{B2}$$

Appendix C: Relaxation time of the optimal engine via master equation

1. Consider a system with $n \gg 1$ degenerate (excited) levels with energy $\varepsilon > 0$, and a single ground state with energy 0. In this section we shall estimate the relaxation time of this system within the Markov master-equation framework. We start with simplifying assumptions for showing the origin of a long relaxation time in this system. We then demonstrate the result at more general level.

Let $\{p_i\}_{i=0}^n$ be the probability of energy levels. The master equation reads

$$\dot{p}_0 = \sum\nolimits_{i=1}^{n} w_{0i}p_i - p_0\sum\nolimits_{i=1}^{n} w_{i0}, \tag{C1}$$

where w_{0i} is rate of the transition $i \to 0$. Since all energy levels besides the lowest one have the same energy ε, the detailed balance condition reads (which reflects the fact that the bath is in equilibrium at temperature $1/\beta$):

$$w_{0i}e^{-\beta\varepsilon} = w_{i0}. \tag{C2}$$

2. Let us now assume that in (C1) all the excited energy levels are equivalent, and hence

$$w_{0i} = w_{01} \quad \text{and} \quad w_{i0} = w_{10}, \tag{C3}$$

do not depend on i' (this assumption is relaxed at the end of the section):

$$\dot{p}_0 = -w_{01}p_0[ne^{-\beta\varepsilon} + 1] + w_{01}, \tag{C4}$$

meaning that the relaxation time τ_r for $p_0(t)$ to converge exponentially to its equilibrium value

$$p_0^{[\mathrm{eq}]} = 1/(1 + ne^{-\beta\varepsilon}) \tag{C5}$$

reads

$$1/\tau_r = w_{01}[ne^{-\beta\varepsilon} + 1]. \tag{C6}$$

A popular choice for the rate is given by the transition state theory [1]:

$$w_{01} = \frac{\kappa}{n+1}\,e^{-\beta(\varepsilon^* - \varepsilon)}, \tag{C7}$$

where $\varepsilon^* > \varepsilon$ is the transition state energy: once the system gets at that state, it has equal probability to move to any state; hence the factor $\frac{1}{n+1}$ in (C7). Here κ does not depend on n; it is determined by the the energy landscape in the vicinity of the transition state and the excited state.

In our situation

$$e^{-\beta\varepsilon} = \mathcal{O}(\ln[n]/n) \quad \text{or} \quad e^{-\beta\varepsilon} = \mathcal{O}(\frac{1}{n\ln[n]}). \tag{C8}$$

Eqs. (C7, C6) then imply that the relaxation time τ_r is roughly (neglecting logarithmic factors)

$$\tau_r = \mathcal{O}(n) \gg 1. \tag{C9}$$

This conclusion is then based on two physical aspects: first that there are many states with the same energy [the factor $\frac{\kappa}{n+1}$ in (C7)]. Second is that the energy gap is large; see (C8).

3. For more general (than the transition state theory) choices of w_{01} we still shall obtain the same result if we require that for any excited state energy $\varepsilon > 0$, (C4) produces a well-defined and finite limit for $n \to \infty$. This request is based on two hidden assumptions: *i)* the master equation is derived within the weak-coupling assumption, hence it cannot contain very fast (in the limit $n \to \infty$) characteristic times; *ii)* the limit $n \to \infty$ can be

taken independently from ε. Now we naturally get that w_{01} and w_{10} have an overall dependence $\mathcal{O}(\frac{1}{n})$:

$$w_{01} = \hat{w}_{01}(\varepsilon)/n, \quad w_{10} = \hat{w}_{10}(\varepsilon)/n, \tag{C10}$$

where $\hat{w}_{10}(\varepsilon)$ and $\hat{w}_{01}(\varepsilon)$ can depend on energy ε, but they do not depend on n directly [cf. (C7)]. Then (C6) assumes a finite limit for $n \gg 1$. We now get from (C10, C8):

$$1/\tau_{\rm r} = \hat{w}_{01}(\varepsilon) \times \mathcal{O}(\frac{1}{n}). \tag{C11}$$

It is natural to assume that for $\varepsilon \to \infty$, $\hat{w}_{01}(\varepsilon)$ stays at least bounded [cf. (C7, C8)], and then we are back to (C9). There is an important relaxation scenario (going back to Arrhenius and improved by Kramers) where $\hat{w}_{01}$ does not depend on ε (provided that $\varepsilon > 0$ is sufficiently large); it is given by $\hat{w}_{01} \propto e^{-\beta V}$, where $V > 0$ is the barrier height [1].

Thus we note that the conclusion (C9) on long characteristic times is not completely straightforward and—if taken out of the usual relaxation theories, e.g. the transition state theory or the Arrhenius theory—it requires several hidden assumptions. In section V of this supplementary material we show that (C9) is violated, and the relaxation time can be much shorter, if allow the system-bath interaction to depend on the system features.

4. Finally, let us return to (C3) and show that this assumption can be relaxed without changing our main conclusions. For a sufficiently large energy gap $\varepsilon > 0$ between the ground state and the excited state, we can apply the adiabatic approximation meaning that the excited levels probability equilibrate between themselves much quicker than the ground state level probability. Hence they all get into the same value:

$$p_i(t) = (1 - p_0(t))/n, \tag{C12}$$

before $p_0(t)$ start to change appreciably. Employing (C12) in (C1) we revert to (C1), where now instead of w_{01} we should employ $\frac{1}{n}\sum_{i=1}^{n} w_{0i}$. Note that (C12) is especially plausible in our situation, since we also start the relaxation process from equilibrium states at a temperature different from the bath temperature. At such an initial state the probabilities of the excited levels are equal.

5. To go beyond the adiabatic approximation we will now consider the whole master equation. Let us first note that the detailed balance conditions (C2) for the transition rates w_{ij} between excited levels lead to $w_{i\neq j} = w_{ji}$; and write down the rest of the master equation (C1)

$$\dot{p}_i = \sum_{j\neq i} w_{ij} p_j - \sum_{j\neq i} w_{ji} p_i - w_{0i} p_i + w_{i0} p_0 \tag{C13}$$

in the following form:

$$\dot{p}_i = \sum_j \bar{w}_{ij} p_j - w_{0i} p_i + e^{-\beta\varepsilon} w_{0i} p_0. \tag{C14}$$

Where the matrix $\bar{w}$ is defined as: $\bar{w}_{ii} = -\sum_{j\neq i} w_{ij}$, $\bar{w}_{i\neq j} = w_{ij}$; and is a symmetric matrix satisfying $\sum_i w_{ij} = 0$ for $\forall j$ and can be shown to be non-positive.

We now form the quantities $Q_i = p_i - e^{-\beta\varepsilon} p_0$, for which the master equation (C1, C14) produces

$$\dot{Q}_i = \sum_j \bar{w}_{ij} Q_j - w_{0i} Q_i - e^{-\beta\varepsilon} \sum_j w_{0j} Q_j. \tag{C15}$$

Introducing the positive and symmetric matrix $W_{ij} = -\bar{w}_{ij} + \delta_{ij} w_{0i}$ and bra-ket notation for vectors, we rewrite (C15) as

$$\frac{d}{dt}|Q\rangle = -\left(W + e^{-\beta\varepsilon}|1\rangle\langle w|\right)|Q\rangle, \tag{C16}$$

where $\langle 1| = (1, ..., 1)$ and $\langle w| = (w_{01}, ..., w_{0n})$. In the equilibrium state $Q_i = 0$.

Now the relaxation time of the system can be estimated via the minimal eigenvalue $\omega_{\rm min}$ of the matrix $W + e^{-\beta\varepsilon}|1\rangle\langle w|$. Below, we show numerically that in the asymptotic limit of $n \to \infty$,

$$\omega_{\rm min} = \left(1 + n e^{-\beta\varepsilon}\right) \frac{\sum_i w_{0i}}{n} + \frac{f_n}{n^2}, \tag{C17}$$

$$f_n = \mathcal{O}\left(1\right), \tag{C18}$$

where f_n does not depend on n for a sufficiently large n. Hence for $n \gg 1$ we neglect the last term in (C17) and obtain for the relaxation time:

$$\frac{1}{\tau_{\rm r}} = \left(1 + n e^{-\beta\varepsilon}\right) \frac{\sum_i w_{0i}}{n}, \tag{C19}$$

confirming that conditions (C10, C8) imply the relaxation time to grow proportionally with n. Eq. (C19) is the same result as was obtained above via the adiabatic approximation. Hence this approximation holds up to the second-order term of the asymptotic expansion of $\omega_{\rm min}$ in terms of n.

We now demonstrate (C17) numerically. As it suggests, it holds also when $e^{-\beta\varepsilon}$ depends on n as in formulas (C8). We present our numerical evidence for an illustrative case of $e^{-\beta\varepsilon} = {\rm const}/n$. Note, that all w_{0i}s and w_{ij}s scale as $1/n$ as in (C10). To prove (C17) we calculated f_n for random collections of nw_{0i}s and nw_{ij}s with various probability distributions; see Table C for illustration.

Appendix D: Relaxation time of sub-optimal engines via adiabatic approximation of the master equation

We return to (C1), but we do not assume anymore that the excited levels $\varepsilon_1, ..., \varepsilon_n$ have the same energy. But we still assume that the gap $\varepsilon_1 > 0$ between the zero-energy ground state and the first excited state is the largest energy parameter in the system, because we want to ensure that the equilibrium ground-state probability is close to

TABLE II: Statistics for f_n – the mean $\langle f_n\rangle$, and standard deviation $\left\langle (f_n-\langle f_n\rangle)^2\right\rangle^{1/2}$ – are shown for different values of n; see (C17, C18). It is seen that both depend on n very weakly.
The Boltzmann weight $e^{-\beta\varepsilon}=0.2/n$. The positive transition probabilities $\hat{w}_{ij}=nw_{ij}=nw_{ji}$ and $\hat{w}_{0k}=nw_{0k}$ are random variables. They are all independent from each other. $\hat{w}_{ij}$ and $\arcsin[\hat{w}_{0k}]$ are uniformly distributed in the interval $(0,1)$. The arcsin function for generating $\hat{w}_{0i}$ is chosen with no special reason (other functions were tried as well with similar results), it is just taken to make distributions different.

n	$\langle f_n\rangle$	$\left\langle (f_n-\langle f_n\rangle)^2\right\rangle^{1/2}$
130	0.147179	0.009826
150	0.149095	0.010866
175	0.146339	0.009440
200	0.147149	0.009600
230	0.147958	0.008707

1. Thus we may apply to (C1) the adiabatic approximation assuming that on those times where p_0 changes, the excited-state probabilities p_i already equilibrated:

$$p_i(t)=(1-p_0(t))e^{-\beta\varepsilon_i}\Big/\sum\nolimits_{i=1}^{n}e^{-\beta\varepsilon_i}\ . \qquad \text{(D1)}$$

Hence the relaxation time $\tau_{\rm r}$ of p_0 deduced from (C1, D1) reads

$$\frac{1}{\tau_{\rm r}}=\frac{\sum_{i=1}^{n}w_{0i}e^{-\beta\varepsilon_i}}{\sum_{i=1}^{n}e^{-\beta\varepsilon_i}}+\sum\nolimits_{i=1}^{n}e^{-\beta\varepsilon_i}w_{0i}, \qquad \text{(D2)}$$

where the employed the detailed balance condition.

Eq. (D2) reproduces the relaxation time of the Zwanzig model [14] [given by (27) of the main text], if we employ the energy spectrum (21) [of the main text] and note that the transition probabilities from the first excited (ζN-degenerate) energy level are constants, $w_{0k}=10^9$ for $k=1,...,\zeta N$, while no transitions (to the ground state) is possible from other excited states: $w_{0l}=0$ for $l=\zeta N+1,...,n$. Here 10^9 is the characteristic microscopic scale [14]. Putting these into (D2) we get that the first term in the right-hand-side of (D2) reproduces (27) of the main text. The second term is negligible, if $e^{-\beta\varepsilon_1}$ is sufficiently small.

Note that according to (27) of the main text, the relaxation time of the Zwanzig model is still unacceptably large, if $N\gg 1$. It is possible to get rid of this restriction, but doing so is not useful for the engine functioning.

Appendix E: A short reminder on the protein folding theory in the context of the Levinthal's paradox

The purpose of this section is to introduce the reader into some of the current ideas in protein folding theory. In particular, this should prevent confusions on how specifically we employ the Levinthal's paradox in our study.

1. Early experiments have shown that proteins can fold (i.e. reach the native, functional state) in a reasonably short time; see [2]. Moreover, they do so spontaneously (without external guidance) and starting from different initial conditions. These experiments created what is known to be the modern thermodynamic paradigm on the protein folding: the native state corresponds to the (relatively) unique global minimum of free energy [2].

2. It however still remained unclear how specifically proteins fold, i.e. what is their kinetics. Levinthal assumed that all unfolded states (conformations) are more or less equivalent [3]. Hence during the relaxation to the folded state all possible conformations are tried out to find the energetically most favorable one. This will take an enormous amount of time, because for a (hypothetical) small protein with 100 residues, the number of possible unfolded states would be about 3^{100} [3]. Since this conclusion is clearly unsupportable (hence the Levinthal's paradox), there should be some structure in the set of unfolded states that makes them non-equivalent.

3. One (by now classical) view suggests that in the course of its relaxation the protein passes through a unique path of partially unfolded intermediate states [4]. They allow stepwise folding, drastically reducing the scale of conformational search. In that view—which was supported by experiments on sufficiently long proteins [4]—the protein folding problem is reduced to relaxation in a finite number of states [2]. Still it was unclear how the protein reaches one of those intermediates, since now the Levinthal's paradox can be reformulated with respect to partial relaxation.

4. In addition to the latter objection, experiments on short proteins have shown that folding intermediates are absent. Hence a new view emerged that explains the protein folding kinetics as taking place on a funnel (free) energy landscape, where different unfolded states have different (free) energies and it is this difference that drives the protein towards the minimum (free) energy state [5, 14]. An example of the above scenario is provided by the Zwanzig's model [14], as reviewed above.

Still for realistic proteins the Zwanzig's model is clearly oversimplified, e.g., it does not include conformational entropy, disorder, residue sequence, *etc.* Thus for a deeper understanding of the protein folding one should go to more realistic models [5], which however share the two main points of the the Zwanzig's model: *i)* unfolded states have different (free) energies; *ii)* the folding time can be made finite via fine-tuning only for sufficiently short proteins having $100-200$ coarse-grained degrees of freedom. It is argued that longer proteins will fold hierarchically, i.e. first certain domains will fold independently from each other (these domains thus play the role of folding intermediates), and only after that the protein will

relax globally. The existence of fine-tuning is explained via evolution, a notorious solver of difficult problems in biology [2].

Appendix F: Fast relaxation scenario

We shall now study a quantum model of relaxation that achieves a fast relaxation of the work-optimal engine at the cost of introducing specific system-bath interaction Hamiltonian.

1. System-bath interaction

Consider a system E with n excited energy levels and one lowest energy (ground state) whose energy we set to zero. All n excited levels have the same energy ϵ.

The initial density matrix of E is Gibbsian at temperature $T_0 = 1/\beta_0$:

$$\rho \propto e^{-\beta_0 H} = r\mathcal{P}_0 + \frac{1-r}{n}\mathcal{P}_\epsilon, \tag{F1}$$

$$r = \frac{1}{1+ne^{-\beta_0\epsilon}}, \tag{F2}$$

where $\mathcal{P}_0 = |0\rangle\langle 0|$ is the projector on the ground state, and $\mathcal{P}_\epsilon$ is the projectors on the n-dimensional eigen-space of ρ with eigenvalue ϵ.

Now E interacts with an external thermal bath at temperature $T = 1/\beta$, so that the density matrix of E converges in time to $\rho_{eq} \propto e^{-\beta H}$. We shall design a concrete model for this interaction and estimate the relaxation time.

We assume that the bath consists of a large number of independent particles prepared in identical (thermal states). E interacts with one particle, then with the second one *etc.* Since the particles are independent, it will suffice to consider the interaction of E with the first particle B only.

We assume that the bath particle B has (among other energies) energy levels E and $E+\varepsilon$. The degeneracies of these levels are n_E and $n_{E+\varepsilon}$, respectively. The initial (before interacting with E) equilibrium density matrix of B reads

$$\sigma = e^{-\beta H_{\rm B}}/Z = \widetilde{\sigma} + r_E\,\Pi_E + r_{\epsilon+E}\,\Pi_{\epsilon+E}, \tag{F3}$$

$$r_E = e^{-\beta E}/Z, \quad Z = \sum\nolimits_E n_E e^{-\beta E}, \tag{F4}$$

where r_E and $r_{E+\varepsilon}$ are the Boltzmann weights for the energy levels E and $E+\varepsilon$, respectively, the summation in (F4) is taken over all energy levels of B. Π_E and $\Pi_{\varepsilon+E}$ are the projectors on the corresponding sub-spaces,

$$\mathrm{tr}\,\Pi_E = n_E, \qquad \mathrm{tr}\,\Pi_{\varepsilon+E} = n_{E+\varepsilon}, \tag{F5}$$

and where $\widetilde{\sigma}$ in (F3) is the remainder of σ.

It is assumed that the unitary operator $\mathcal{V}$ responsible for the interaction operates within the sub-space with the projector $\mathcal{P}_\varepsilon\otimes\Pi_E + \mathcal{P}_0\otimes\Pi_{E+\varepsilon}$ (this sub-space has energy $E+\varepsilon$), i.e.,

$$[\,\mathcal{V}, \mathcal{P}_\varepsilon\otimes\Pi_E + \mathcal{P}_0\otimes\Pi_{E+\varepsilon}\,] = 0. \tag{F6}$$

On the remainder of the overall Hilbert space (of E+B) $\mathcal{V}$ acts as unit operator. Thus, $\mathcal{V}$ commutes with the Hamiltonian of E+B. Hence no additional energy (work) is needed for switching the E-B interaction on and off. In that respect $\mathcal{V}$ resembles the weak-coupling, though by itself it need not be weak, i.e. it need not be smaller than the Hamiltonian of E+B.

Then the post-interaction density matrix ρ' of E reads

$$\begin{aligned}\rho' &= \mathrm{tr}_{\rm B}\mathcal{V}\rho\otimes\sigma\mathcal{V}^\dagger \\ &= \rho - \left(r\,r_{E+\varepsilon} - r_E\,\frac{1-r}{n}\right)\times \\ &\quad [n_{E+\varepsilon}\mathcal{P}_0 - \mathrm{tr}_{\rm B}\mathcal{V}\mathcal{P}_0\otimes\Pi_{E+\varepsilon}\mathcal{V}^\dagger].\end{aligned} \tag{F7}$$

It will suffice to keep track of the lowest energy-level occupation $\langle 0|\rho'|0\rangle \equiv r'$ only:

$$r' - r = -A\,[r - r_{\rm eq}]\,, \quad r_{\rm eq} \equiv \frac{1}{1+ne^{-\beta\varepsilon}}, \tag{F8}$$

$$A \equiv \frac{r_E}{r_{\rm eq}n}\left[n_{E+\varepsilon} - \langle 0|\,(\,\mathrm{tr}_{\rm B}\mathcal{V}\mathcal{P}_0\otimes\Pi_{E+\varepsilon}\mathcal{V}^\dagger\,)|0\rangle\right], \tag{F9}$$

where $r_{\rm eq}$ is the equilibrium value of r. Using (F4) one can show that $A \le A_{\max} \le 1$: after the interaction E gets closer to its equilibrium state; see (F8).

Now (F7) serves as the initial state of E for a similar interaction with the second bath particle that initially has the same state σ as in (F3). We get for all subsequent interactions [we revert from (F10) to (F8) for $m = 1$]:

$$r^{[m]} - r_{\rm eq} = (1-A)^m\,[r - r_{\rm eq}]\,, \tag{F10}$$

It is seen that (F10) predicts exponential (with respect to the number of collisions) relaxation towards the equilibrium value $r_{\rm eq}$ of r. The approach to equilibrium is governed by the factor $(1-A)^m$ meaning that when $|A| \ll 1$ the effective number of interactions after which the equilibrium is established (which is proportional to the relaxation time) equals to $-1/[\ln(1-A)]$.

2. Minimization of the relaxation time

Since we are interested in possibly shorter relaxation time, we need to maximize A over the unitary $\mathcal{V}$ [under condition (F6)]. To do that, we first write $P_0\otimes\Pi_{E+\varepsilon}$ in a conveniently chosen matrix form in the energy eigenbasis

$$P_0\otimes\Pi_{E+\varepsilon} = \tag{F11}$$

$$\mathrm{diag}(\underbrace{...,1,...,1,...}_{n_{E+\epsilon}\text{ elements}}|\underbrace{...,0,...,0,...}_{n\text{ sections}}|\cdots|...,0,...,0,...), \tag{F12}$$

where sections correspond to eigenvectors of H, and elements in sections run over the ones of H_B. Values are

shown only for the subspace given by $P_0\otimes\Pi_{E+\varepsilon}+P_\varepsilon\otimes\Pi_E$. The first section (denoted as $|...|$) there are $n_{E+\varepsilon}$ unities. Then come n identical sections, each one contains n_E zeroes.

To maximize A we need to minimize $\langle 0|\,(\,\mathrm{tr_B}\mathcal{V}\mathcal{P}_0\otimes\Pi_{E+\varepsilon}\mathcal{V}^\dagger\,)|0\rangle$ over all possible $\mathcal{V}$s living in $P_0\otimes\Pi_{E+\varepsilon}+P_\varepsilon\otimes\Pi_E$. One can show that the optimal unitary amounts to a permutation of the eigenvalues (F12) (this fact can be shown similarly to the derivation presented in (9–12) of the main text). Now we note that the trace over tr_B amounts to summing up elements in each section. So the element $\langle 0|\,(\,\mathrm{tr_B}\mathcal{V}\mathcal{P}_0\otimes\Pi_{E+\varepsilon}\mathcal{V}^\dagger\,)|0\rangle$ will be the sum of the elements of the first section in the permuted diagonal in (F11). The optimal permutation will thus be the one which takes out of the first section as much unities as possible. Therefore, if $n_{E+\varepsilon}$ (the number of unities) is $<$ than n_En—the number of zeroes—then it is possible to move all unities, making $\min_{\mathcal{V}}\left\{\langle 0|\,(\,\mathrm{tr_B}\mathcal{V}\mathcal{P}_0\otimes\Pi_{E+\varepsilon}\mathcal{V}^\dagger\,)|0\rangle\right\}=0$. Otherwise, the latter quantity will be $n_{E+\varepsilon}-n_En$, leading us to the following formula:

$$A_{\max}=\frac{r_E\min\left[\,n_{E+\varepsilon},n_En\,\right]}{r_{\mathrm{eq}}n}. \tag{F13}$$

3. One-shot relaxation

Now the shortest relaxation corresponds to just one collision and it is reached for $A=1$, e.g., $r_E^{[1]}=r_{\mathrm{eq}}$ and $n_{E+\varepsilon}^{[1]}=n-1$ in (F13). Then the corresponding unitary operator $\mathcal{V}$ is the SWAP operation. The relaxation time in this case amounts to one inter-collision time.

However, in this case the bath should consist of particles that have the same energy gap as the system. This is not a realistic model for the bath. Below we study a fully realistic bath model and show that although the relaxation time in that situation is larger than a single collision time, it still allows to conclude that the Carnot efficiency can be reached at a large power.

4. Relaxation time for realistic bath

Let us work out (F13) for a realistic example of the bath. We assume that the bath particle amounts to $L\gg 1$ independent two-level systems. Each such system has energies 0 and ζ. Thus the bath particle has energies $0,\zeta,2\zeta,...,L\zeta$. Each bath energy level E is degenerate

$$n_E=\frac{L!}{(E/\zeta)!(L-E/\zeta)!} \tag{F14}$$

times. Provided that

$$n_{E+\varepsilon}>n_En, \tag{F15}$$

we obtain

$$A_{\max}=(1+ne^{-\beta\epsilon})\,\frac{n_Ee^{-\beta E}}{Z}. \tag{F16}$$

Since we want a larger $A_{\max}$, we take

$$E=L/(e^{\beta\zeta}+1). \tag{F17}$$

Hence using the Stirling's formula $L!\simeq\sqrt{2\pi L}\,L^Le^{-L}$ and noting that $Z=(1+e^{-\beta\zeta})^L$ we get from (F16)

$$A_{\max}\simeq(1+ne^{-\beta\epsilon})\sqrt{\frac{1+e^{-\beta\zeta}}{L}}. \tag{F18}$$

We work out (F15) via the Stirling's formula and obtain from (F15, F17)

$$\frac{\ln[n]}{L}+h_2[\frac{1}{e^{\beta\zeta}+1}]<h_2[\frac{1}{e^{\beta\zeta}+1}+\frac{\epsilon}{L\zeta}], \tag{F19}$$

where $h_2[x]=-x\ln x-(1-x)\ln(1-x)$.

Let us specify ϵ as [μ is a parameter]

$$\epsilon=\mu T\ln[n],\quad \mu>1. \tag{F20}$$

Putting this into (F19) we get

$$\frac{\ln[n]}{L}+h_2[\frac{1}{e^{\beta\zeta}+1}]<h_2[\frac{1}{e^{\beta\zeta}+1}+\frac{\mu}{\beta\zeta}\,\frac{\ln[n]}{L}]. \tag{F21}$$

Provided that $\mu>1$, (F21) can be satisfied for sufficiently small (but finite) $\frac{\ln[n]}{L}$ and sufficiently large $\zeta>0$. Note that (F21) never holds for $\mu\leq 1$.

Returning to (F18) we see from (F20) that for $\ln[n]=\mathcal{O}(L)\gg 1$

$$A_{\max}=\mathcal{O}(\frac{1}{\sqrt{\ln[n]}}), \tag{F22}$$

which means that the relaxation time scales as $\mathcal{O}(\sqrt{\ln[n]})$.

Consider now the opposite [to (F15)] case

$$n_{E+\varepsilon}<n_En, \tag{F23}$$

where

$$A_{\max}=(1+\frac{1}{ne^{-\beta\epsilon}})\,\frac{n_{E+\epsilon}e^{-\beta(E+\epsilon)}}{Z}. \tag{F24}$$

Choosing

$$E+\epsilon=L/(e^{\beta\zeta}+1), \tag{F25}$$

we get [cf. (F18)]

$$A_{\max}\simeq(1+\frac{1}{ne^{-\beta\epsilon}})\sqrt{\frac{1+e^{-\beta\zeta}}{L}}. \tag{F26}$$

If we specify [cf. (F20)]

$$\epsilon=\nu T\ln[n],\quad \nu<1, \tag{F27}$$

then (F23) reads [cf. (F21)]

$$h_2[\frac{1}{e^{\beta\zeta}+1}]<\frac{\ln[n]}{L}+h_2[\frac{1}{e^{\beta\zeta}+1}-\frac{\nu}{\beta\zeta}\,\frac{\ln[n]}{L}]. \tag{F28}$$

This relation holds for $\nu<1$, sufficiently small (but finite) $\frac{\ln[n]}{L}$ and sufficiently large $\zeta>0$.

Hence from (F28, F24) we return to the same conclusion (F22).

5. Relations with the main text

In the main text—see in particular (16, 19)— we studied the relaxation of the optimal engine E that has the energy spectrum described at the beginning of section IV. More specifically, in the main text we needed two different relaxation scenario: E with energy gap $\epsilon^{[1]} \simeq T_1 \ln[n]$ relaxes on a thermal bath at temperature T_2 (where $T_1 > T_2$), and conversely E with energy gap $\epsilon^{[2]} \simeq T_2 \ln[n]$ relaxes on a thermal bath at temperature T_1; see (18) of the main text in this context.

Now the first case corresponds to (F20, F21, F22), while the second case to (F27, F28, F22). In both cases we get that for a realistic thermal bath (but with tuned system-bath interactions) the relaxation time amounts to $\mathcal{O}(\sqrt{\ln[n]})$; see (F22).

Appendix G: Entanglement generation during relaxation

It is important to understand to which extent quantum are the polynomial-time relaxation mechanisms discussed above. First of all, how much system-bath entanglement has to be generated in the course of relaxation? Recall that entanglement is an essentially quantum resource and a sizable amount of entanglement would pose an additional limitation on approaching the Carnot limit. Such additional limitations are likely to be absent, as we demonstrate below.

Note that though the collisional relaxation scheme do not assume any entanglement between the system and bath particle both before and after the collision, it can still imply that some amount of entanglement is generated during the collision. Nevertheless, in $\ln n \to \infty$ limit (where the machine achieves the Carnot limit for the efficiency) the amount of entanglement goes to zero linearly with $\ln n$; recovering, thus, the classical nature of our setup in thermodynamic limit.

The fact that the system and bath get entangled during the relaxation (especially in the mesoscopic regime) implies that the dynamics of the system is non-Markovian [12].

Since the simplest case, the one-shot relaxation (see section (F 3)), has all the traits of the phenomenon, we will show the above assertion on that particular example.

Say in the first relaxation step the system E starts with the diagonal state $\rho = \frac{1}{1+nu_1}\,\mathrm{diag}(1, u_1, ..., u_1)$ and with hamiltonian $H_2 = \mathrm{diag}(0, \varepsilon^{[2]}, ..., \varepsilon^{[2]})$. Where u_1 and u_2 (and, through it, $\varepsilon^{[2]}$) are determined from Eq. (16) of the main text. The whole relaxation process is but a SWAP operation between E and one bath particle B which has the same hamiltonian H_2 and is in a thermal state with bath temperature T: $\sigma_B = \frac{1}{1+nu_2}\,\mathrm{diag}(1, u_2, ..., u_2)$.

The relaxation progresses autonomously – no energy flow in or out happens (otherwise one would need a third system to accept/give energy and a control to switch on and off the interactions, while the relaxation is supposed to be a probably prearranged but a spontaneous process). To that end, the interaction between E and B, H_{EB}, must satisfy [9]

$$[H_{EB},\, H_E \otimes 1_B + 1_E \otimes H_B] = 0. \tag{G1}$$

Hence for H_{EB} to be nontrivial it must act within the direct sum $\mathcal{H}_{\mathcal{D}}$ of two nonintersecting degenerate subspaces of $H_E \otimes 1_B + 1_E \otimes H_B$ (the one spanned on eigenvectors with energy $\varepsilon^{[2]}$ and the other – on eigenvectors with energy $2\varepsilon^{[2]}$). The unitary preforming SWAP also lives in that subspace, and, thus, can be generated by a suitably chosen H_{EB}. So the relaxation is executed by a one-parametric continuous family of unitaries $U(t)$ that live in $\mathcal{H}_{\mathcal{D}}$ and satisfy

$$U(0) = 1, \quad U(t_{rel}) = \mathrm{SWAP} \tag{G2}$$

where t_{rel} is the duration of the collision=relaxation time.

Now, we introduce the following quantity

$$E = \min_{U(t)} \left\{ \max_{t} \left[\mathcal{N}\left(U(t)\rho \otimes \sigma_B U^{\dagger}(t) \right) \right] \right\}; \tag{G3}$$

where $\mathcal{N}$ is the entanglement negativity [10, 11], which measures the entanglement between the systems.

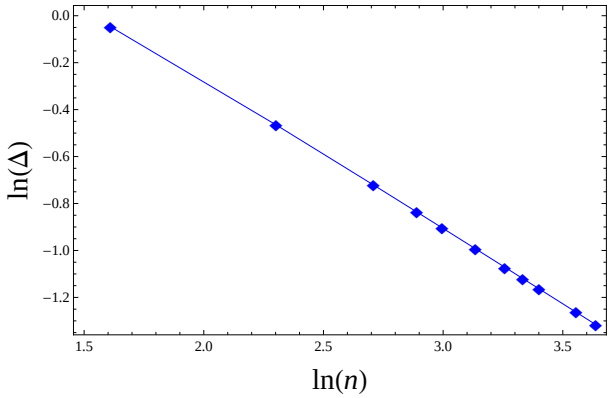


FIG. 1: The dependence of $\ln(\Delta(n, T_1))$ on $\ln(n)$ for $T_1 = 2$. The dependence is linear within the numerical errors. The slope of the line $b \approx 0.65$; hence $\Delta(n, T_1) \sim n^{-b}$.

The quantity E in (G3) indicates the very necessity of entanglement generation, since it finds the maximum over a process and then takes the minimum of the maxima over all processes consistent with constraints (G2). So if it is zero, then one can find a process which proceeds without entangling the system and the bath particle, while if it is positive, any process will reach a point during its runtime when it starts to entangle the parties involved. Note that when calculating E we do not take into direct account the constraint generated by (G1).

As applied to our problem, we determine the quantities $u_{1,2}(n, T_1, T_2)$ from Eq. (16) of the main text, then plug the resulting states ρ and σ_B in (G3) and perform

the min-max optimization. The resulting quantity is the indicator (G3) as a function of n, T_1, and T_2 (denote it by $E_o = E_o(n, T_1, T_2)$).

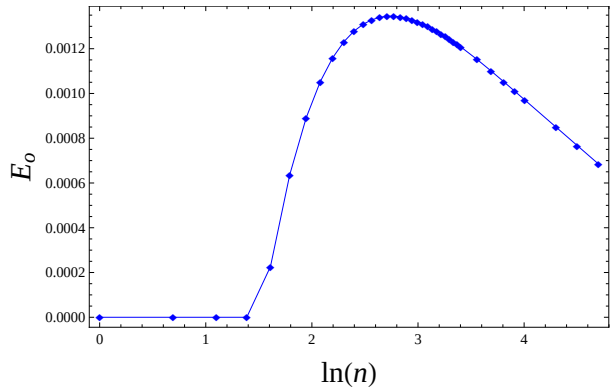


FIG. 2: The dependence of $E_o(n, T_1, T_2)$ on $\ln(n)$ for $T_1 = 2$, $T_2 = 1$. As is clearly seen, the dependence becomes linear for $n \gtrsim 30$.

There is no entanglement when $T_2 = T_1$ since the states ρ and σ_B become identical and the SWAP does not alter them so that the joint state remains constant and factorized. There the minimal eigenvalue of the partially transposed density matrix is strictly positive, so the continuity implies that there is a whole interval $(T_1 - \Delta(n, T_1), T_1)$ of T_2 that $E_o(n, T_1, T_2) = 0$. This is indeed certified by the numerics which also enables to calculate the interval length Δ as a function of n and T_1. It turns out, that for any fixed T_1, Δ decreases with n. Also, the numerical data (see Fig. (1)) suggest that $\Delta \to 0$ as $n \to \infty$.

If we now fix the temperatures of the baths and calculate the $E_o(n, T_1, T_2)$ as a function of n, we will indeed see that for small n's there is no negativity. Then, starting from some n, it starts to appear and grow. But unexpectedly the negativity passes through a maximum and starts to decrease linearly with $\ln n$ (see Fig. (2)). So, as $\ln n \to \infty$, the necessity to generate entanglement drops out. The latter is the limit where the engine's efficiency approaches the Carnot value. So in the asymptotic limit we have both $\eta \to \eta_C$ and $E_o \to 0$ for any $T_2 < T_1$; where the latter means that although entanglement is necessarily generated during the relaxation for almost any unequal temperatures of baths, its amount goes to zero so that the dynamics becomes essentially classical.

[1] H-X. Zhou, Quarterly Reviews of Biophysics **43**, 219 (2010).

[2] P. Echenique, *Introduction to protein folding for physicists*, arXiv:0705.1845.

[3] C. Levinthal, *How to fold graciously*, in Mossbauer Spectroscopy in Biological Systems, edited by J. T. P. DeBrunner and E. Munck, pp. 2224 (Allerton House, Monticello, Illinois, 1969, University of Illinois Press).

[4] R.L. Baldwin, Protein Sci. **6**, 2031 (1997).

[5] P.G. Wolynes, Phil. Trans. R. Soc. A **363**, 453 (2005).

[6] L.D. Landau and E.M. Lifshitz, *Statistical Physics, I*, Pergamon Press Oxford, 1978.

[7] K. Sekimoto, F. Takagi, and T. Hondou, Phys. Rev. E **62**, 7759 (2000).

[8] K. Sekimoto and S. Sasa, J. Phys. Soc. Jpn. **66**, 3326 (1997).

[9] A.B. Brailovskii, V.L. Vaks, and V.V. Mityugov, Phys. Usp. **166**, 745 (1996).

[10] G. Vidal and R.F. Werner, Phys. Rev. A **65**, 032314 (2002).

[11] Negativity is the sum of negative eigenvalues of the joint density matrix after a partial transposition. When it is positive then one knows for sure that there is some entanglement present, while one cannot guarantee that there is no entanglement when it is zero.

[12] S. Shresta, C. Anastopoulos, A. Dragulescu, and B.L. Hu, Phys Rev. A **71**, 022109 (2005).